First La Plata International School, 2008
Compact Object and their Emission, 2009
Ileana Andruchow & Gustavo E. Romero, eds.

High-energy emission from low-mass microquasars

Gabriela S. Vila[1] & Gustavo E. Romero[1,2]

[1] *Instituto Argentino de Radioastronomía (IAR-CCT La Plata-CONICET), C.C.5, 1894 Villa Elisa, Buenos Aires, Argentina. gvila@iar-conicet.gov.ar*

[2] *Facultad de Ciencias Astronómicas y Geofísicas, UNLP, Paseo del Bosque s/n, 1900 La Plata, Buenos Aires, Argentina.*

Abstract. Microquasars are binary systems with a compact object accreting from a donor star, characterised by the presence of relativistic jets. The electromagnetic spectra of microquasars can range from radio to gamma-rays. In this work we explore the possibility of obtaining high-energy emission from microquasars where the donor star is a low-mass, old and dim star without strong winds. We propose that the interaction of relativistic particles with radiation and magnetic fields in the jet can be an efficient channel of gamma-ray production in such systems. We focus particularly in proton-dominated jets. We develop a simple model to characterise the jet and the distribution of relativistic particles in steady state. We then calculate the emission spectrum due to different processes: synchrotron radiation, inverse Compton scattering and proton-photon interaction. The contribution of secondary leptons is also estimated. Our results indicate that, under some conditions, low-mass microquasars might be gamma-ray sources detectable by high-energy instruments like GLAST.

1. Introduction

There exists a group of variable gamma-ray sources in the galactic halo whose nature still remains unidentified. They are located at high galactic latitudes, typically from 2 to 8 kpc, and they present variability on all time scales. The luminosity of these sources in gamma-rays is in the range $\sim 10^{33-36}$ erg/s, 10-100 times higher than their luminosity in X-rays. They display soft spectra, with spectral indices ~ 2.5 (if S_γ is the measured photon flux, then $S_\gamma \propto E_\gamma^{-2.5}$). Among the possible counterparts of some of these halo sources are low-mass microquasars (LMMQs). Microquasars are binary systems composed by a black hole accreting from a companion star. They present jets of relativistic particles. In the case of a LMMQ, the donor star is a low-mass, old and dim star, without strong winds. The microquasar scenario can account for several of the general characteristics of the halo sources. The rapid variablity observed in these sources implies the presence of a compact object, and it is known that microquasars might be the site of efficient particle acceleration and high-energy emission, as demonstrated by the detection of three of them at TeV energies (Aharonian et al. 2005; Albert et al. 2006; Albert et al. 2007). LMMQs in particular, have

large proper motions and they can be found outside the galactic plane (Mirabel et al. 2001; Ribó et al. 2002). An example is XTE J1118+480, the firmest black hole candidate in the galactic halo.

Several models have been proposed for the production of gamma-rays in LMMQs. Grenier et al. (2005) developed a model based on inverse Compton scattering (IC) of external photon fields by relativistic leptons in the jets. The photons are provided by the star, and the accretion disk and the corona of hot plasma that surround the black hole. However, in a LMMQ these fields are too weak for this mechanism to explain the observed luminosities. As an alternative, synchrotron self-Compton (SSC) interactions were considered by Aharonian & Atoyan (1998), Atoyan & Aharonian (1999) and Bosch-Ramon et al. (2006). In this case, the target photons for IC scattering are produced by the same electrons in the jet through synchrotron radiation. Models based on hadronic interactions were introduced as well. Romero et al. (2003) studied the production of gamma-rays in LMMQs through proton-proton inelastic collisions between relativistic protons in the jet and the matter field of the wind of the star. Photohadronic interactions were introduced in the context of microquasars by Levinson & Waxman (2001).

In this work we propose that high-energy electromagnetic emission in low-mass microquasars can be produced through the interaction of relativistic leptons and hadrons with the radiation field and the magnetic field in the jet, and not with external fields. We develop a simple model of jet, obtain the distribution of relativistic particles, and calculate the emission spectra taking into account several radiation processes. Finally, we asses the possible detection of these sources by future gamma-ray instruments.

2. Jet model

We consider a conical jet, launched perpendicular to the orbital plane. It is injected at a distance $z_0 \approx 10^8$ cm from the compact object, where z is the jet axis. The jet radius grows as $r(z) = r_0(z/z_0)$, with $r_0 = 0.1z_0$. The outflow is only mildly relativistic, with a bulk Lorentz factor of $\Gamma_{\rm jet} = 1.5$. We assume that a fraction $q_{\rm jet} = 0.1$ of the accretion luminosity $L_{\rm accr} = 2 \times 10^{39}$ erg s^{-1} powers the jet, $L_{\rm jet} = q_{\rm jet} L_{\rm accr}$. This energy is divided between the relativistic hadrons and leptons that populate the jet, $L_{\rm jet} = L_p + L_e$. We relate the energy budget of both species as $L_p = aL_e$. Since we want to study proton-dominated jets, we only consider the case $a \geq 1$.

Although not completely understood, the mechanism of ejection of the jets is thought to be magnetohydrodynamic. If this is the case, there must be at least as much energy stored in the magnetic field as kinetic energy in the plasma that is being ejected. Therefore, the magnetic field at the base of the jet can be estimated assuming equipartition of energy between the magnetic energy density and the kinetic energy density of the jet at z_0, $U_B(z_0) = U_{\rm kin}(z_0)$. The value of $B_0 = B(z_0)$ can be obtained from the relation

$$\frac{B_0^2}{8\pi} = \frac{L_{\rm jet}}{\pi r_0^2 v_{\rm jet}}, \qquad (1)$$

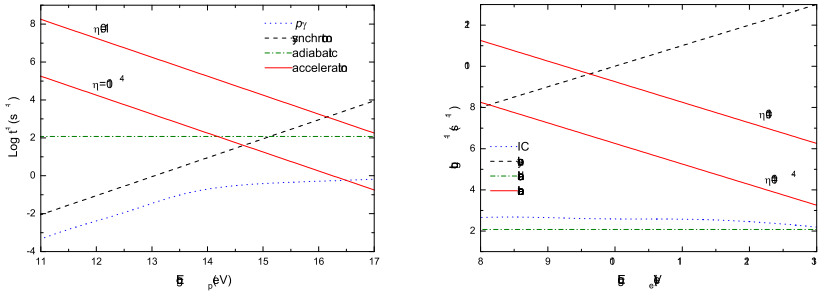

Figure 1. Acceleration and cooling rates at the base of the jet for protons (left panel) and electrons (right panel), calculated for representative values of the model parameters ($E^{\rm min} = 100\,mc^2$, $a = 1$ and $\alpha = 2.2$).

where $v_{\rm jet}$ is the jet's bulk velocity. This yields a value of $B_0 \approx 10^7$ G. For $z > z_0$, the magnetic field decays as the jet expands,

$$B(z) = B_0 \frac{z_0}{z}. \tag{2}$$

The acceleration of particles takes place in a compact region that extends from z_0 to $z_{\rm max} = 5z_0$. Relativistic particles are injected at a rate

$$Q = Q_0 \frac{E^{-\alpha}}{z} \qquad\qquad [\mathrm{Q}] = \mathrm{erg}^{-1}\mathrm{cm}^{-3}\mathrm{s}^{-1}. \tag{3}$$

Diffusive shock acceleration naturally leads to this type of power-law injection function. We consider two different values for the spectral index, $\alpha = 1.5$ and $\alpha = 2.2$, hard and soft injection spectrum, respectively. The z-dependence in Eq. 3 was added to take into account that the injection is reduced as the distance from the compact object increases.

The maximum energy of a relativistic particle in the jet can be estimated equating the acceleration rate and the rate of cooling, $t_{\rm acc}^{-1} = t_{\rm cool}^{-1}$. The acceleration rate for a particle of charge e in a magnetic field B is given by

$$t_{\rm acc}^{-1} = \eta ceBE^{-1}. \tag{4}$$

The parameter η characterises the efficiency of the acceleration. We studied two cases, $\eta = 0.1$ and $\eta = 10^{-4}$, that describe a very efficient and a poor acceleration, respectively.

Particles lose energy through adiabatic and radiative losses, $t_{\rm cool}^{-1} = t_{\rm ad}^{-1} + t_{\rm rad}^{-1}$. As can be seen from Fig. 1, the main radiative process of energy loss is synchrotron radiation, with a cooling rate

$$t_{\rm synchr}^{-1} = \frac{4}{3}\left(\frac{m_e}{m}\right)^3 \frac{c\sigma_T U_B}{m_e c^2}\frac{E}{mc^2}. \tag{5}$$

This is the only relevant cooling channel for electrons. For protons, adiabatic losses must also be taken into account,

$$t_{\rm ad}^{-1} = \frac{2}{3}\frac{v_{\rm jet}}{z}. \tag{6}$$

We obtain a maximum proton energy of $E_p^{\rm max} \sim 10^{17}\eta^{1/2}$ eV, whereas for electrons $E_e^{\rm max} \sim 3 \times 10^{10}\eta^{1/2}$ eV.

The distibution in energy of the relativistic particles, $N(E,z)$ (erg^{-1} cm^{-3}), was calculated as in Khangulyan et al. (2007), solving the transport equation in steady state in the "one-zone" approximation,

$$\frac{\partial}{\partial E}\left[\left.\frac{dE}{dt}\right|_{\rm cool} N\left(E,z\right)\right] + \frac{N\left(E,z\right)}{t_{\rm esc}} = Q\left(E,z\right). \tag{7}$$

Here, $dE/dt|_{\rm cool} = Et_{\rm cool}^{-1}$, and $t_{\rm esc} = z_{\rm max}/v_{\rm jet}$ is the particle escape time from the acceleration region. This equation describes an homogeneus jet, and it is valid as long as the acceleration region is compact. The resulting distributions have a power-law dependence in the particle energy. For protons, N_p mimics the injection function, $N_p \propto E_p^{-\alpha}$; for electrons strong synchrotron losses produce a break in the spectrum, and $N_e \propto E_e^{-(\alpha+1)}$.

3. Radiative processes

We consider three contributions to the emission spectrum: synchrotron radiation of primary protons and primary and secondary leptons, leptonic inverse Compton scattering and photohadronic interactions.

The synchrotron spectra is calculated using standard formulae, as can be found for example in Blumenthal & Gould (1970). The power radiated by a single particle of energy E, mass m and charge e is given by

$$P_{\rm synchr}\left(E_\gamma, E, z, \alpha\right) = \frac{\sqrt{3}e^3 B(z)}{4\pi mc^2 h}\frac{E_\gamma}{E_{\rm c}}\int_{E_\gamma/E_{\rm c}}^{\infty} {\rm d}\xi\, K_{5/3}(\zeta). \tag{8}$$

Here E_γ is the energy of the emitted photon, α is the pitch angle (angle between the particle momentum and the magnetic field), and $K_{5/3}(\zeta)$ is a modified Besell function. Most of the energy is radiated in photons of energy near the characteristic value E_c,

$$E_{\rm c} = \frac{3heB(z)\sin\alpha}{4\pi mc}\left(\frac{E}{mc^2}\right)^2. \tag{9}$$

The total power $L_{\rm synchr}\left(E_\gamma\right)$ radiated by an isotropic distribution of particles $N(E,z)$ can then be found as

$$L_{\rm synchr}\left(E_\gamma\right) = E_\gamma \int_V {\rm d}^3 r \int_{\Omega_\alpha} {\rm d}\Omega_\alpha \sin\alpha \int_{E^{\rm min}}^{E^{\rm max}(z)} {\rm d}E\, N(E,z)\, P_{\rm synchr}. \tag{10}$$

The inverse Compton scattering of synchrotron photons by leptons yields a second contribution to the emission spectrum. For a single electron of energy

$E_e = \gamma_e m_e c^2$ in a photon field of density $n\left(\epsilon, z\right)$, the IC emissivity is (Blumenthal & Gould 1970)

$$P_{\rm IC}\left(E_\gamma, E_{\rm e}, \epsilon, z\right) = \frac{3\sigma_{\rm T} c}{4\gamma_{\rm e}^2} \frac{n\left(\epsilon, z\right)}{\epsilon} F\left(q\right). \tag{11}$$

Here $\sigma_{\rm T}$ is the Thomson cross section, and the function $F(q)$ is given by

$$F\left(q\right) = 2q\ln q + \left(1+2q\right)\left(1-q\right) + \frac{1}{2}\left(1-q\right)\frac{\left(q\Gamma_{\rm e}\right)^2}{\left(1+\Gamma_{\rm e}q\right)}, \tag{12}$$

where $\Gamma_{\rm e} = 4\epsilon\gamma_{\rm e}/m_{\rm e}c^2$ and $q = E_\gamma/[\Gamma_{\rm e}E_{\rm e}\left(1 - E_\gamma/E_{\rm e}\right)]$. These expressions are valid even in the Klein-Nishina regime ($\Gamma_e \gg 1$), where the relativistic lepton losses most of its energy in a single collision. The total IC luminosity $L_{\rm IC}(E_\gamma)$ can be calculated as in Eq. (10), integrating in the energy E_e of the electrons and in the energy ϵ of the target photons.

Synchrotron photons also serve as a target field for photohadronic ($p\gamma$) interactions. This process has two main branches: photopair and photomeson production. Photopair production,

$$p + \gamma \rightarrow p + e^- + e^+, \tag{13}$$

was studied among others by Chodorowski et al. (1992), Mücke et al. (2000) and Mastichiadis et al. (2005). In the δ-functional approximation, where each lepton is created with an energy $E_{e^\pm} \sim (m_e/m_p)E_p$, the pair emissivity can be written as

$$\begin{aligned} Q_{e^\pm}\left(E_{e^\pm}, z\right) &= 2\int {\rm d}E_p N_p\left(E_p, z\right)\omega_{p\gamma,\,e^\pm}\left(E_p\right)\delta\left(E_{e^\pm} - \frac{m_e}{m_p}E_p\right) \\ &= 2\frac{m_p}{m_e}N_p\left(\frac{m_p}{m_e}E_{e^\pm}\right)\omega_{p\gamma,\,e^\pm}\left(\frac{m_p}{m_e}E_{e^\pm}\right). \end{aligned} \tag{14}$$

In this expression $N_p(E_p, z)$ is the proton distribution and $\omega_{p\gamma,\,e^\pm}$ is the collision rate,

$$\omega_{p\gamma,\,e^\pm}(\gamma_p) = \frac{c}{2\gamma_p^2}\int_{\frac{\epsilon_{\rm th}}{2\gamma_p}}^{\infty} {\rm d}\epsilon \frac{n\left(\epsilon\right)}{\epsilon^2}\int_{\epsilon_{\rm th}}^{2\epsilon\gamma_p} {\rm d}\epsilon' \sigma_{p\gamma,\,e^\pm}\left(\epsilon'\right)\epsilon'. \tag{15}$$

In our case, $n(\epsilon)$ is the density of the synchrotron photon fields. The threshold energy is $\epsilon_{\rm th} \sim 1$ MeV, and we use the parametrization of the cross section $\sigma_{p\gamma,\,e^\pm}$ given by Maximon (1968).

Photomeson production procceds via two main branches with approximately the same probability,

$$p + \gamma \rightarrow p + a\pi^0 + b\left(\pi^+ + \pi^-\right) \tag{16}$$

and

$$p + \gamma \rightarrow n + \pi^+ + a\pi^0 + b\left(\pi^+ + \pi^-\right), \tag{17}$$

followed by the decays

$$\pi^+ \rightarrow \mu^+ + \nu_\mu, \quad \mu^+ \rightarrow e^+ + \nu_\mathrm{e} + \overline{\nu}_\mu, \tag{18}$$

$$\pi^- \rightarrow \mu^- + \overline{\nu}_\mu, \quad \mu^- \rightarrow e^- + \overline{\nu}_\mathrm{e} + \nu_\mu \tag{19}$$

and

$$\pi^0 \rightarrow 2\gamma. \tag{20}$$

Following Atoyan & Dermer (2003), we calculate the photon and pair emissivity product of the pion decay in the δ-functional approximation,

$$Q_\gamma\left(E_\gamma\right) = 20 N_p\left(10E_\gamma\right) \omega_{p\gamma,\,\pi}\left(10E_\gamma\right) n_{\pi^0}\left(10E_\gamma\right), \tag{21}$$

$$Q_{e^\pm}\left(E_{e^\pm}\right) = 20 N_p\left(20E_{e^\pm}\right) \omega_{p\gamma,\,\pi}\left(20E_{e^\pm}\right) n_{\pi^\pm}\left(20E_{e^\pm}\right). \tag{22}$$

The collision rate $\omega_{p\gamma,\,\pi}$ is given by (14) with the cross section replaced by the correspondent for photomeson production, and n_{π^0} and $n_{\pi^\pm}$ are the mean number of π^0 and $\pi^\pm$ created per proton-photon interaction, respectively. Expressions for all this quantities can be found in Atoyan & Dermer (2003).

All the expressions given above are valid in the comoving reference frame of the jet. To transform them to the observer frame, we must take into account the viewing angle θ and the Lorentz factor of the jet Γ_jet, through the Doppler factor D,

$$D = \frac{1}{\Gamma_\mathrm{jet}\left(1 - \beta_\mathrm{jet}\cos\theta\right)}. \tag{23}$$

Energies and luminosities in the comoving (primed) and the observer (non-primed) frames are then related as

$$E_\gamma = D E'_\gamma \tag{24}$$

and

$$L_\gamma\left(E_\gamma\right) = D^2 L'_\gamma\left(E'_\gamma\right). \tag{25}$$

We fix a moderate value for the viewing angle, $\theta = 30\,\mathrm{deg}$. None of the results depend strongly on this value as long as Γ_jet remains small.

4. Results and discussion

Figure 2 shows some of the calculated spectral energy distributions (SEDs). Proton synchrotron radiation yields a peak in the spectrum around 10 GeV or 10 MeV, depending on the efficiency of the acceleration η, that in turn fixes the proton maximum energy. This component can reach luminosities of $\sim 10^{37}$

erg s^{-1}, almost independently of the value of a. The synchrotron spectra of primary leptons does depend on a, since these particles radiate almost all their energy budget, reaching luminosities in the range $10^{37} - 10^{34}$. Different spectral shapes are obtained depending on the injection spectral index α. The decay of neutral pions and the synchrotron radiation of secondary leptons created through $p\gamma$ collisions contribute to the SEDs at very high energies, up to 10^{16} eV for $\eta = 0.1$. The three contributions are of the same order of magnitude. In any case IC scattering is relevant.

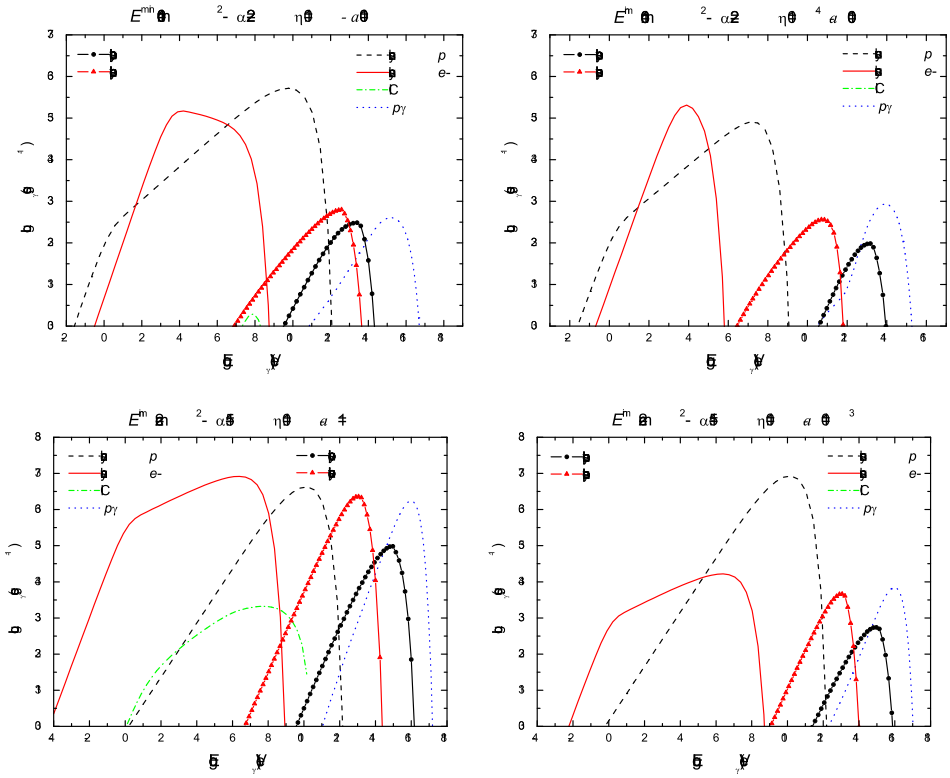

Figure 2. Spectral energy distributions obtained for different values of the parameters.

Since the proton synchrotron peak is always below 1 TeV, its detection by ground-based Cherenkov telescopes is difficult. This componenent might be detected by future gamma-ray satellites like GLAST, that operates in the range 100 MeV to 300 GeV. In cases like the one in the bottom left panel of Fig. 2, however, the contribution of secondary leptons could be detectable by HESS II and MAGIC II. Neutrinos of energies above 1 TeV, a by-product of our model through photomeson production, can also be expected with a luminosity similar to that of the high-energy tail of the calculated SEDs. It is important to note that internal photon-photon absorption can introduce modifications in the production spectra, particularly in cases with a high lepton component ($a = 1$). High-energy photons are very effectively absorbed in the synchrotron field of

primary electrons, leading to the supression of the emission above 10 GeV. For detailed results on this aspect, see Romero & Vila (2008).

5. Conclusions

We have showed that, under certain physical conditions, low-mass microquasars can be efficient gamma-ray sources. This opens up the possibility that some of the unidentified sources in the galactic halo can belong to this class of objects. In future works, we expect to improve our model including refinements in the radiative calculations (see for example Kelner et al. 2008 for the case of $p\gamma$ interactions). We will also go beyond the one-zone model, to achieve a more consistent description of the particle distributions. Finally, we expect to introduce time dependence effects to try to reproduce the observed variability. Observations with forthcoming gamma-ray instruments wil de useful to contrast our predictions, and will contribute with new data that can help to constrain the model parameters.

References

Aharonian, F. A., & Atoyan, A. M. 1998, New Astron. Rev., 42, 579
Aharonian, F. A., et al. 2005, Science, 309, 746
Albert, J., et al. 2006, Science, 312, 1771
Albert, J., et al. 2007, ApJ, 665, L51
Atoyan, A. M., & Aharonian, F. A. 1999, MNRAS, 302, 253
Blumenthal, G. R. & Gould, R. J. 1970, Rev. Mod. Phys., 42, 237
Bosch-Ramon, V., et al. 2006, A&A, 447, 263
Chodorowski, M. J., et al. 1992, ApJ, 400, 181
Grenier, I. A., Kaufman Bernadó, M. M., & Romero, G. E. 2005, Ap&SS, 297, 109
Khangulyan, D., et al. 2007, MNRAS, 380, 320
Levinson, A., & Waxman, E. 2001, Phys. Rev. Lett., 87, 171101
Mastichiadis, A., et al. 2005, A&A, 433, 765
Maximon, L. C. 1968, J. Res. NBS, 72B, 79
Mirabel, I. F., et al. 2001, Nature, 413, 139
Mücke, A., et al. 2000, Comm. Phys. Comp., 124, 290
Ribó, M. et al. 2002, A&A, 384, 954
Romero, G. E., & Vila, G. S. 2008, A&A, astro-ph 0804.4606
Romero, G. E., et al. 2003, A&A, 410, L1